Measurement of the time alignment between muon detector and calorimeters with the 2008 cosmic runs

LHCb-PUB-2009-028
18/11/2009

LHCb Public Note

Issue: 1
Revision: 0

Reference: LHCb-PUB-2009-028
Created: November 18, 2009
Last modified: November 18, 2009

Prepared by: **M. Frosini**, INFN Sezione di Firenze, Italy

Abstract

The aim of this note is to present some results concerning the time alignment between the LHCb Muon Detector and the Calorimeter system. The analysis is performed by computing the time residuals between the two detectors on a sample of cosmic muons acquired by the experiment during September 2008. To have a more detailed description of the current state of the time alignment, time residuals have been separated according to the station and region of the Muon Detector crossed by the cosmic rays. The estimated misalignment of the Muon Detector with respect to the Electromagnetic Calorimeter is about $4 - 7$ ns while the misalignment with respect to the Hadronic Calorimeter is about $1 - 4$ ns. Using the external time reference provided by the Calorimeters, the R4 region is found to be misaligned with respect to the other regions by about $2 - 3$ ns. This behaviour has been seems to be independent both from the choice among Electromagnetic and Hadronic calorimeter, and from the calorimeter's region intercepted by the tracks.

Contents

1 Introduction

During the LHCb Muon System commissioning cosmic ray tracks are a very important instrument to check the relative time alignment of the detector: in fact, although they don't have a known time origin, they provide full synchronous signals when corrected for the time of flight. To evaluate the time alignment of the Muon Detector with respect to the whole experiment an external system of reference is needed. In particular the time residuals of the Muon Detector have been measured with respect to the Calorimeter system. The data sample consists of cosmic rays from 2008 runs. In section 2 the data sample will be discussed. Sections 3 and 4 provide a brief description of the track reconstruction procedure in the Muon Detector and in the Calorimeters system respectively. To compare the time measurements from the Muon Detector and from the Calorimeters it is necessary to select only particles which have crossed both the detectors: in section 5 we describe the procedure used for matching tracks to the Electromagnetic and Hadronic calorimeters. Finally in section 6 the results will be presented.

2 Data sample

The data sample used for this analysis consists of two sets of cosmic ray runs collected in September 2008. The run conditions are described in details in [1]. The sample corresponds to 8.5×10^5 events with about 2.4×10^5 tracks reconstructed in the muon detector.

3 Track reconstruction and selection in the Muon Detector

The track reconstruction in the Muon Detector is performed in two steps. The first step consists in searching among all the hits those aligned along a straight line. This is done with an algorithm based on a recurrent neural networks implemented within BRUNEL (see [2]). In the second step two linear fit procedures are applied to the selected hits. The first fit provides the space parameters of the track: in particular, the projections of the track on the zx plane and on the yz plane are independently fitted, to obtain the slopes (s_x and s_y) and the intercepts (b_x and b_y) of the two bi-dimensional straight lines. In the second fit procedure the points are interpolated with the quantity

$$t_{TRACK} = t_0 + \frac{\sqrt{(z \cdot s_x)^2 + (z \cdot s_y)^2 + z^2}}{c} \tag{1}$$

with z being the z coordinate of the hit. The quantity t_{TRACK} is the track time, that is the average of the time measurements of the hits belonging to a track, corrected for the time of flight with respect to a reference station which in this analysis was chosen to be M4. The raw hit time was preliminarly corrected with an iterative time–alignment procedure, described in details in [3]. In Fig. 1 the distributions of χ^2 for the fit procedure on zx plane and zy plane are shown. To reject the tracks which were wrongly reconstructed, the following cuts were applied on these quantities:

$$\chi^2_x < 20, \quad \chi^2_y < 20. \tag{2}$$

To select a clean sample of well reconstructed tracks a cut on the number N_{HITS} of hits associated was applied:

$$N_{HITS} < 6, \tag{3}$$

Taking into account that the reconstruction is performed using only M2 to M5 stations (M1 was not yet installed), with this cut all the tracks where cross–talk hits or noise hits are included are rejected, allowing at most an additional hit.

4 Track reconstruction in the Calorimeters

The hit time measurement in the Calorimeters is described briefly in this section; further details can be found in [4]. For each particle crossing the Calorimeter system, the coordinates of the intersection point and the energy deposit are measured. The energy released by the particle in the calorimeter pads is summed over three consecutive bunch crossings (*Prev, T0 and Next*)

$$E_{TOT} = \sum_i \left[E_i(Prev) + E_i(T0) + E_i(Next) \right]. \tag{4}$$

where index i labels each pad. Noise events are subtracted applying two different cuts on E_{TOT} for electromagnetic and hadron calorimeter. In each calorimeter the pad corresponding to the higher energy deposit ($\overline{x}_{ECAL,HCAL}$, $\overline{y}_{ECAL,HCAL}$) is identified. The projection of the track on xy plane is determined by computing the azimuthal angle $\overline{\varphi}_{ECAL,HCAL}$ with the following weighted average

$$\overline{\varphi}_{ECAL,HCAL} = \frac{\sum_i w_i \arctan\left(\Delta y_i / \Delta x_i\right)}{\sum_i w_i} \tag{5}$$

where $w_i = E_i/d_i$, d_i is the distance of the i-th pad from $(\bar{x}_{ECAL,HCAL}, \bar{y}_{ECAL,HCAL})$ and Δx_i and Δy_i are the d_i components along horizontal and vertical direction. This is done for both calorimeters. All the hits whose distance from the straight lines identified by $(\bar{x}_{ECAL,HCAL}, \bar{y}_{ECAL,HCAL})$ and $\overline{\varphi}_{ECAL,HCAL}$ is less than a predefined cut are then selected and their centre of mass is evaluated. The straight line passing through the two centers of mass described above define the xy projection of the track segment in the calorimeters. The polar angle θ is determined by the coordinates z_{ECAL} and z_{HCAL}. Hits time in the calorimeters is not directly measured but is computed from the analysis of the shape of the signal integrated by the preamplifiers. The signal length is about 40 ns and in the ideal case its plateau is centred with respect to the bunch crossing where it can be sampled to give an amplitude proportional to the energy released in the pad. When the signal is shifted with respect to the centre of the bunch crossing, it can be sampled over two consecutive bunch crossings: in this way the energy deposit is measured two times with two different amplitudes. The signal asymmetry over two consecutive bunch crossings is defined as

$$R_j = \frac{\sum_{i=1}^{N_{evt}} E_{ij}(current) - \sum_{i=1}^{N_{evt}} E_{ij}(next)}{\sum_{i=1}^{N_{evt}} E_{ij}(current) + \sum_{i=1}^{N_{evt}} E_{ij}(next)} \tag{6}$$

where N_{evt} is the number of events, $E_{ij}(current)$ and $E_{ij}(next)$ are the energy deposits of the i-th event and in the j-th pad, during the T0 bunch crossing and the Next bunch crossing. The time measurement is finally extrapolated from the asymmetry R_j using a fit procedure.

5 Comparison between Muon System and Calorimeter time measurements

To compare the time measurements in the Muon System and in the Calorimeters, cosmic ray tracks are reconstructed independently in both detectors and then matched together. For this purpose the track reconstructed in the muon detector has been extrapolated on the electromagnetic and on the hadron calorimeter determining the intersection points, respectively $P_{extECAL}$ and $P_{extHCAL}$. On each calorimeter the distance between the measured and the extrapolated point has been computed, giving the residuals

$$\overrightarrow{\Delta r}(ECAL) = \overrightarrow{P}_{ECAL} - \overrightarrow{P}_{extECAL} \tag{7}$$
$$\overrightarrow{\Delta r}(HCAL) = \overrightarrow{P}_{HCAL} - \overrightarrow{P}_{extHCAL}. \tag{8}$$

In Fig. 3 the projection of the residuals along the horizontal direction ($\Delta r_x(ECAL)$ and $\Delta r_x(HCAL)$) is shown versus the projection along the vertical direction ($\Delta r_y(ECAL)$ and $\Delta r_y(HCAL)$). The distributions of the $\overrightarrow{\Delta r}(ECAL)$ and $\overrightarrow{\Delta r}(HCAL)$ components along the x and y direction are superimposed and shown in Fig. 4 and Fig. 5. In each calorimeter the distribution of the vertical component is wider than the distribution of the horizontal one because of the finer granularity of the muon detector along x than along y. Taking into account this behaviour an elliptical cut was applied on $\overrightarrow{\Delta r}(ECAL)$ and $\overrightarrow{\Delta r}(HCAL)$ to select only tracks where

$$\frac{\Delta r_x(ECAL)^2}{a^2_{ECAL}} + \frac{\Delta r_y(ECAL)^2}{b^2_{ECAL}} < 1 \tag{9}$$
$$\frac{\Delta r_x(HCAL)^2}{a^2_{HCAL}} + \frac{\Delta r_y(HCAL)^2}{b^2_{HCAL}} < 1 \tag{10}$$

In this way just the tails of the distributions were rejected.
In Fig. 6 we show the distributions of energy deposit in electromagnetic and hadron calorimeter for tracks selected with the previous cut. Both the distributions are fitted by a Landau function: this ensures that the procedure really selects MIPs.

6 Results and comments

The time alignment has been studied computing the residuals between the time measured by electromagnetic and hadron calorimeters and the time of the track reconstructed in the muon detector and extrapolated to the calorimeters. The sample is composed by the tracks selected with the cuts 9 and 10. The track time has been extrapolated to the calorimeters:

$$t_{TRACK}(z_{ECAL}) = t_0 + \frac{\sqrt{(x \cdot z_{ECAL})^2 + (y \cdot z_{ECAL})^2 + z^2_{ECAL}}}{c} \tag{11}$$
$$t_{TRACK}(z_{HCAL}) = t_0 + \frac{\sqrt{(x \cdot z_{HCAL})^2 + (y \cdot z_{HCAL})^2 + z^2_{HCAL}}}{c} \tag{12}$$

with z_{ECAL} and z_{HCAL} being the positions along the z axis of electromagnetic and hadron calorimeter, respectively. The time residuals are given by

$$r_t(ECAL) = t_{raw}(ECAL) + TOF(M4) - t_{TRACK}(z_{ECAL}) \tag{13}$$
$$r_t(HCAL) = t_{raw}(HCAL) + TOF(M4) - t_{TRACK}(z_{HCAL}). \tag{14}$$

where $TOF(M4)$ is the time of flight with respect to M4, $t_{raw}(ECAL)$ and $t_{raw}(HCAL)$ are the raw time measured by the calorimeters. The residuals were measured separately according to the station and the region of the muon detector crossed by the particle assigning a track to station s and region r if a hit is found in s, r. In this

way for each calorimeter sixteen time residual distributions are obtained. The mean value of each distribution is shown in Fig. 7 and Fig. 8. In these histograms the different regions are numbered from 1 to 16 from M2–R1 to M5–R4. From these plots an average delay of the electromagnetic calorimeter of about $4 - 7$ ns with respect to the muon detector is observed. For the hadron calorimeter the observed delay is about $1 - 4$ ns. Generally the R4 region seems to have a better time alignment with respect to the other regions. To investigate further this effect, the tracks were assigned to a region tracks with more than two hits in different stations of that region. The distributions of time residuals obtained with this selection are shown in Fig. 9 and Fig. 10, for electromagnetic and hadron calorimeter. The misalignment of R4 with respect to the other regions is still visible and it is of about $3 - 4$ ns for electromagnetic calorimeter and $2 - 3$ ns for hadron calorimeter. To check a possible correlation of this misalignment with the intersection point between the track and the calorimeter, the maps of mean time residuals were analysed. The distributions are shown in Fig. 11 and Fig. 12. The results are separated according to the region of muon detector crossed by the tracks. Maps of the electromagnetic calorimeter show the presence of some regions, in particular the right side and the centre, where the time residuals are generally lower than in the remaining surface: this is probably due to a misalignment of these zones of ECAL with respect to the whole calorimeter. This behaviour becomes more evident if the mean time residuals are shown separately versus horizontal and vertical coordinate of the intersection point, as shown in Fig. 13 and Fig. 14. As in the maps of ECAL, the distribution of $r_t(ECAL)$ versus the x coordinate shows a region of the electromagnetic calorimeter ($x_{ECAL} > 3000$ mm) where the time residuals are significantly lower than in the whole calorimeter. In Fig. 15 and Fig. 16 are shown the same distributions for the hadron calorimeter. In all these plots the mean time residuals for tracks coming from R4 region are lower than in the other region. This behaviour seems to be independent from the zone of electromagnetic and hadron calorimeter intercepted by the track and could be due to a delay of R4 with respect to the other regions.

7 Conclusions

In this note, a procedure to mutually time align the Muon Detector and the Calorimeters of LHCb has been described. The procedure is based on the matching of the track segments reconstructed independently by the two subsystem and on the corresponding time measurements. By measuring the residuals between the time of the muon tracks extrapolated to the calorimeters corrected for the time of flight and the raw hit time measured by the calorimeters themselves, a relative time misalignment between the two subdetector has been spotted. Moreover, by selecting tracks crossing different space regions, it is possible to identify possible misalignments between different regions of the two subdetectors. This procedure will provide a powerful tool for the synchronization of the calorimeters and the muon detector once tracks from the interaction point will be available.

8 References

[1] W. Bonivento and G. Manca,*Measurement of the logical pad cluster size of the installed muon chambers with the 2008 cosmic runs*, LHCb Public Note, LHCb-2009-031
`http://cdsweb.cern.ch/record/1163365/files/LHCb-2009-031.pdf`

[2] G. Passaleva, *A recurrent neural network for track reconstruction in the LHCb Muon System*, Nuclear Science Symposium Conference Record, NSS 08 IEEE, pp.867-872 (2008)

[3] W. Bonivento, F. Dettori, G. Manca, R. Oldeman, M. Sireus, G. Graziani, G. Passaleva,*Measurement of the time resolution of the installed muon chambers with the 2008 cosmic runs*, LHCb Public Note, LHCb-PUB-2009-016
`http://cdsweb.cern.ch/record/1207335/files/LHCb-PUB-2009-016.pdf`

[4] Y. Amhis, J. Lefrancois, F. Machefert and MH. Schune, *Proposal for a procedure for the time alignment in the ECAL and HCAL*, LHCb Internal Note, LHCb-2007-146
`http://cdsweb.cern.ch/record/1075723/files/lhcb-2007-146.pdf`

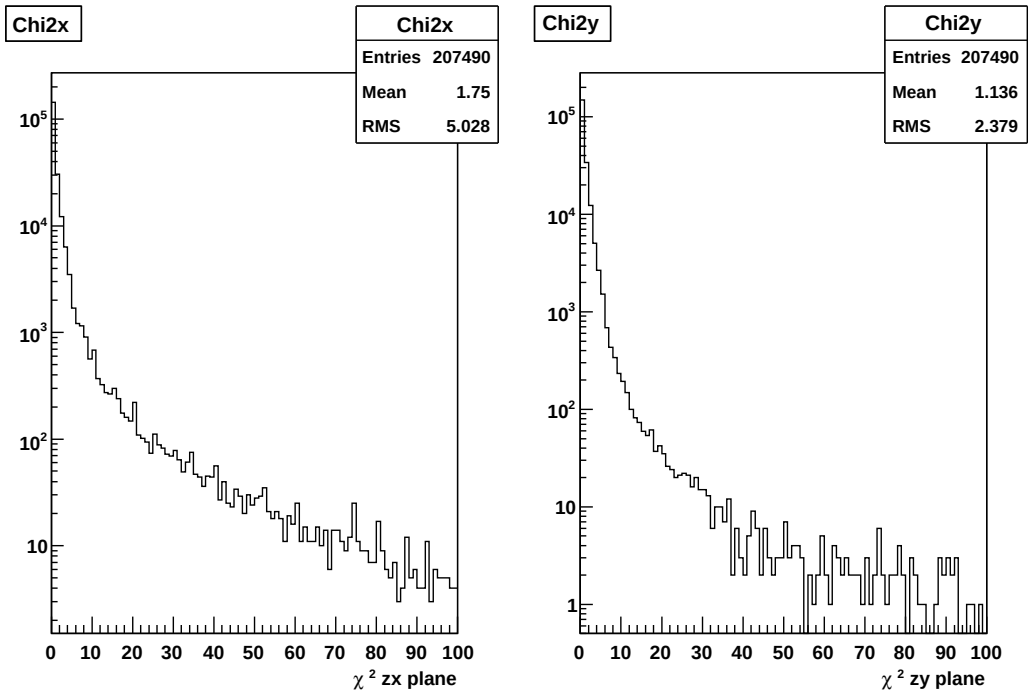

Figure 1 χ^2 distribution for the linear fit on zx plane (right side) and on zy plane (left side).

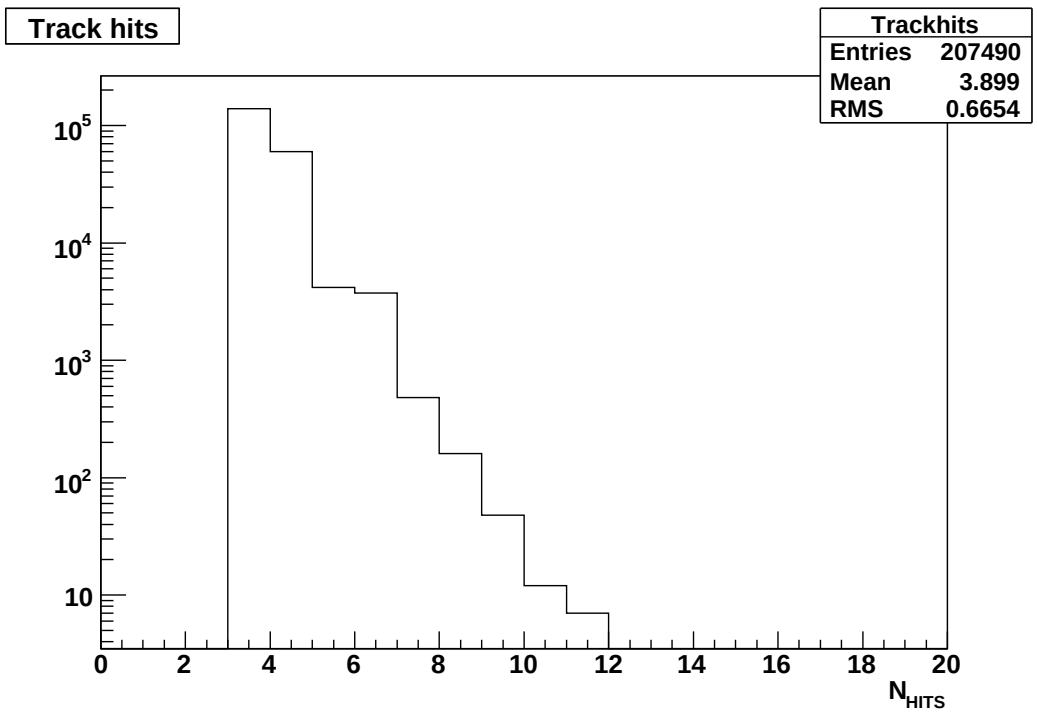

Figure 2 Distribution of N_{HITS}, number of hits belonged to a track.

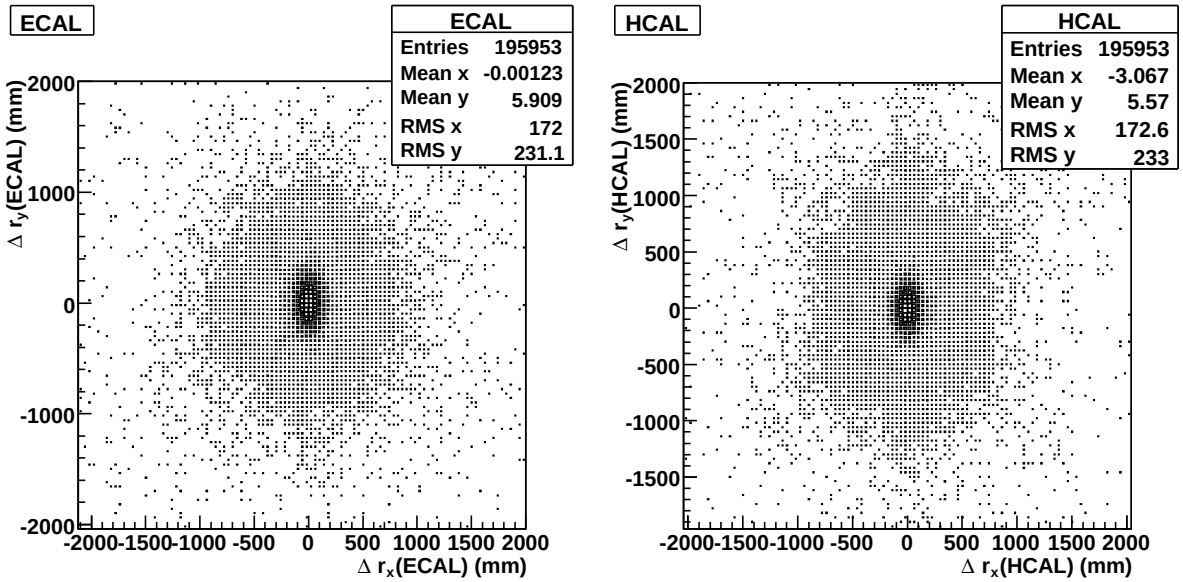

Figure 3 Distribution of residuals between the muon track extrapolation to the calorimeters and the calorimeter reconstructed track segments

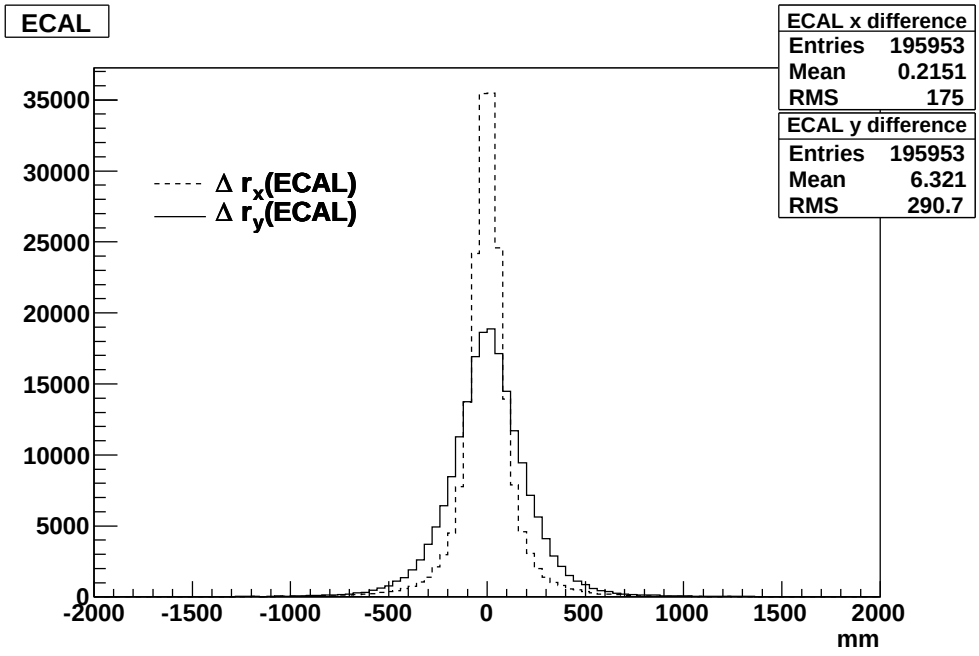

Figure 4 Projection of residuals on electromagnetic calorimeter along horizontal and vertical direction.

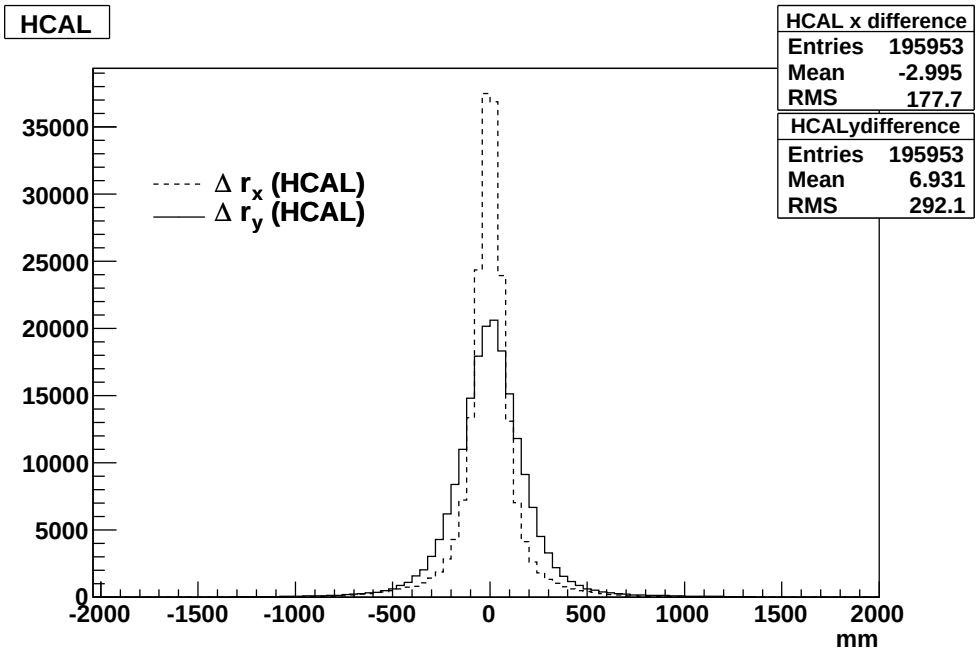

Figure 5 Projection of residuals on hadron calorimeter along horizontal and vertical direction.

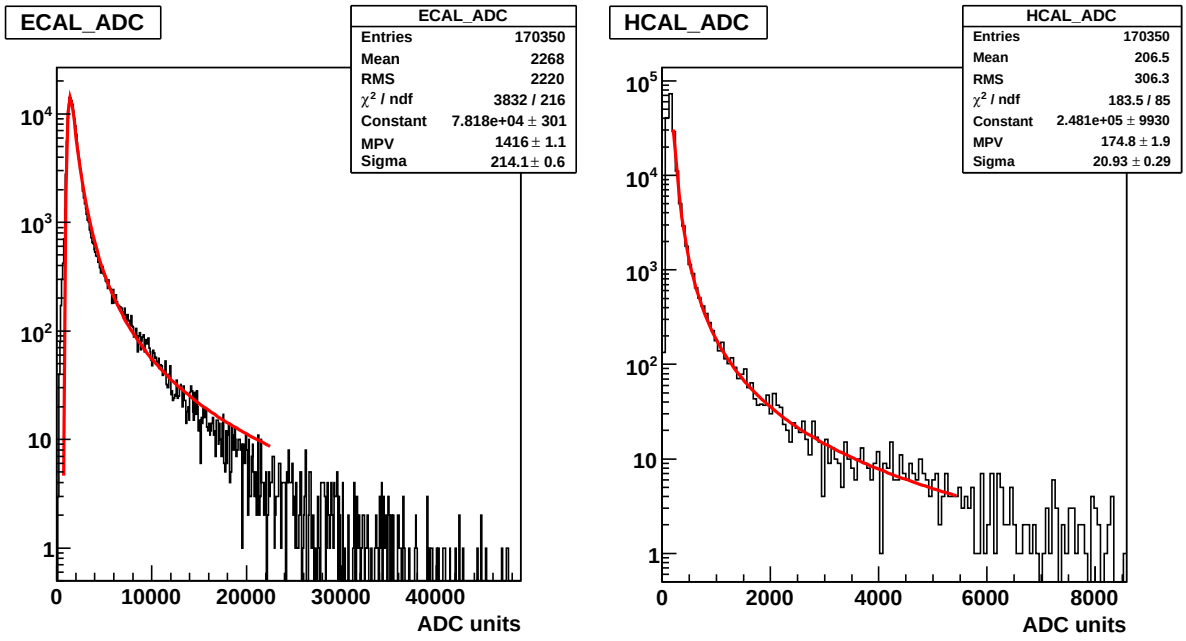

Figure 6 Energy deposit on electromagnetic (left) and hadron calorimeter (right) fitted by a Landau function for tracks selected with cuts 9 and 10 . Energy values are given in ADC units.

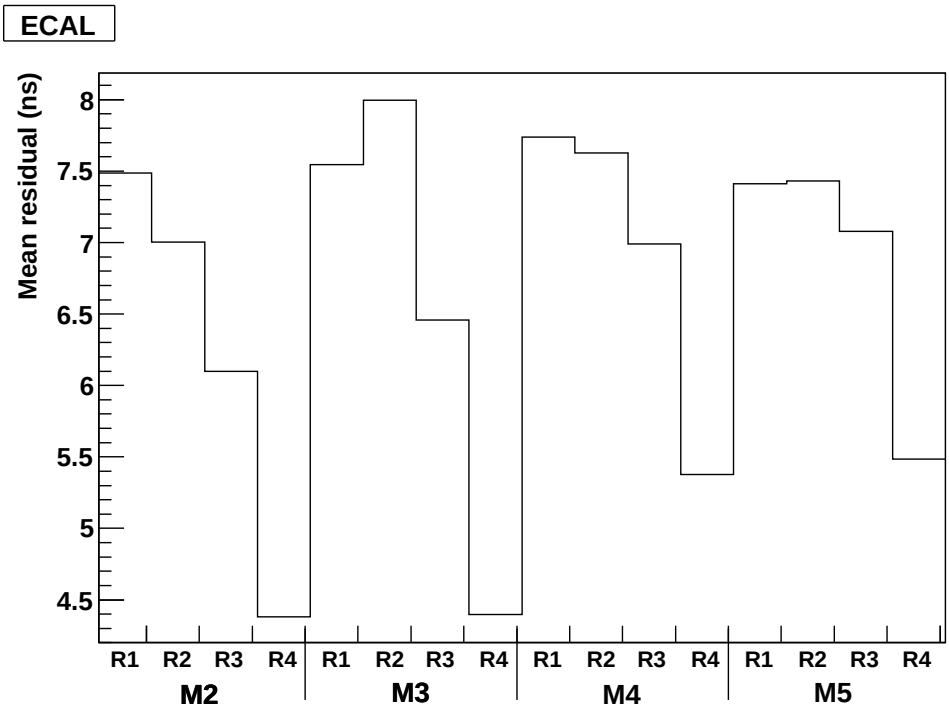

Figure 7 Mean time residual between electromagnetic calorimeter and muon system versus station and region of muon detector crossed by the particle.

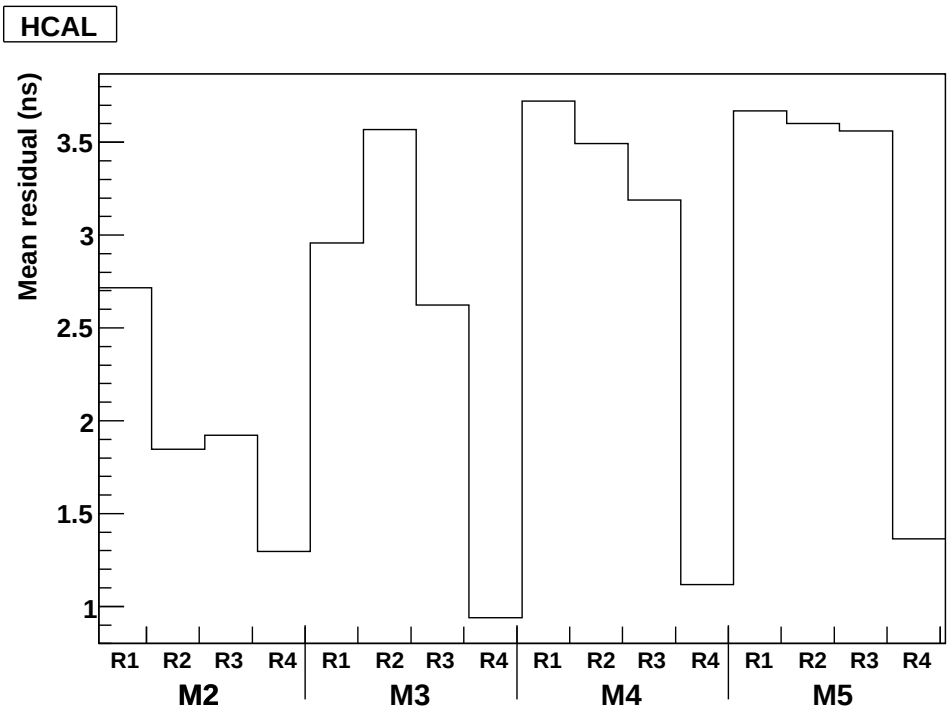

Figure 8 Mean time residual between hadron calorimeter and muon system versus station and region of muon detector crossed by the particle.

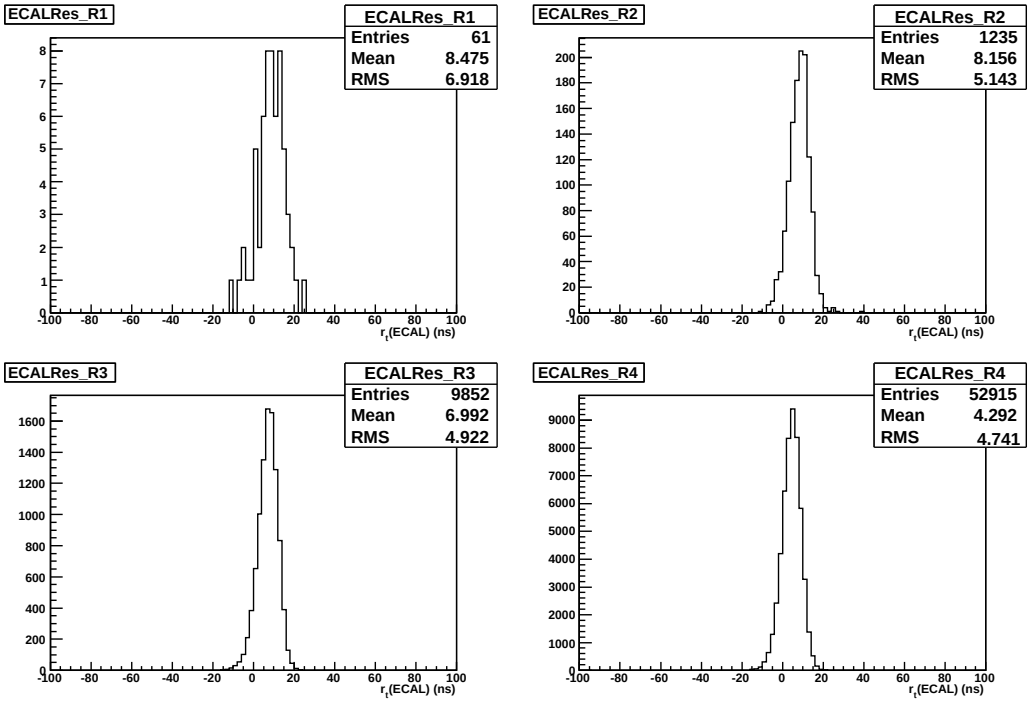

Figure 9 Time residuals distributions between electromagnetic calorimeter and muon detector. Results are separated according to the region of the muon detector crossed by the track.

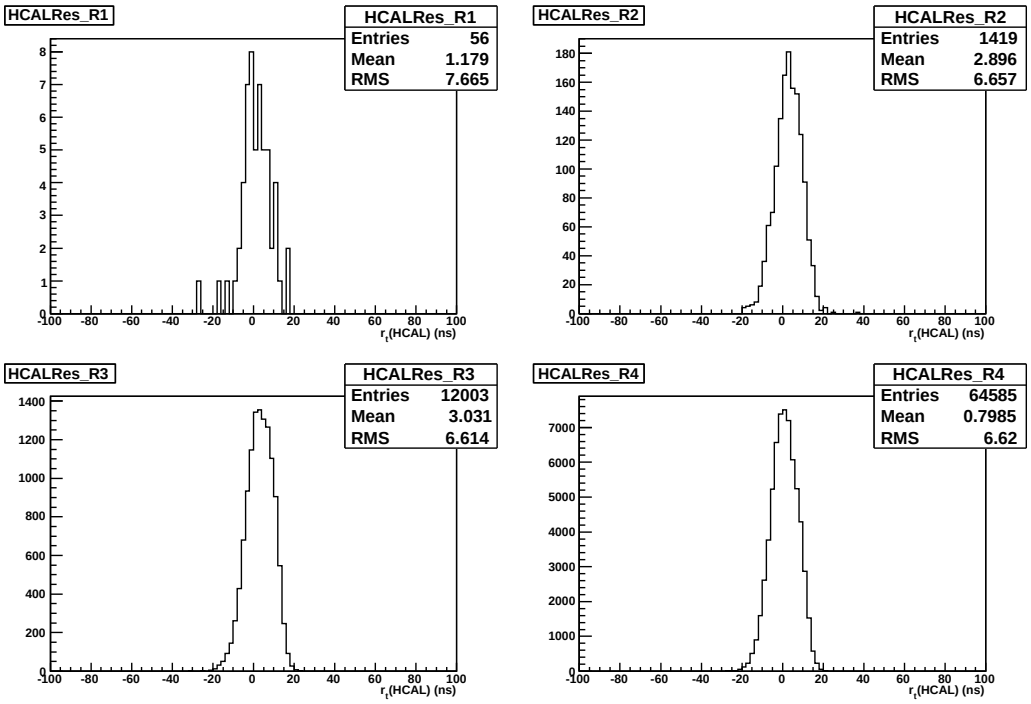

Figure 10 Time residuals distributions between hadron calorimeter and muon detector. Results are separated according to the region of the muon detector crossed by the track.

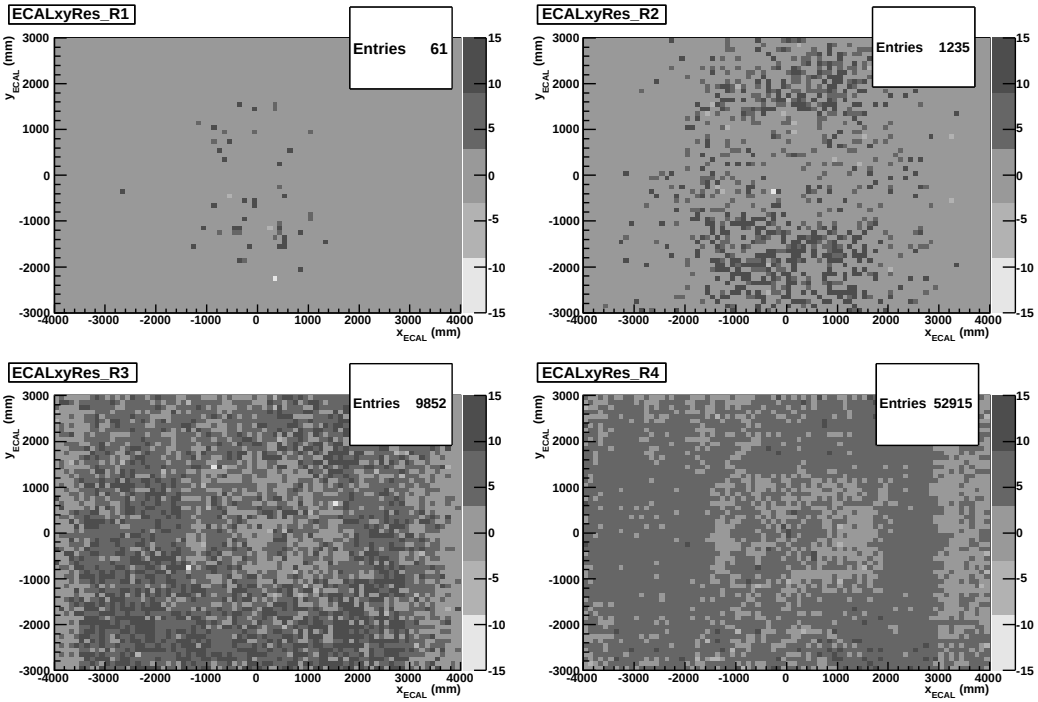

Figure 11 Maps of mean time residuals on electromagnetic calorimeter. Results are separated with respect to the region of muon detector crossed by the track. The color scale is in ns.

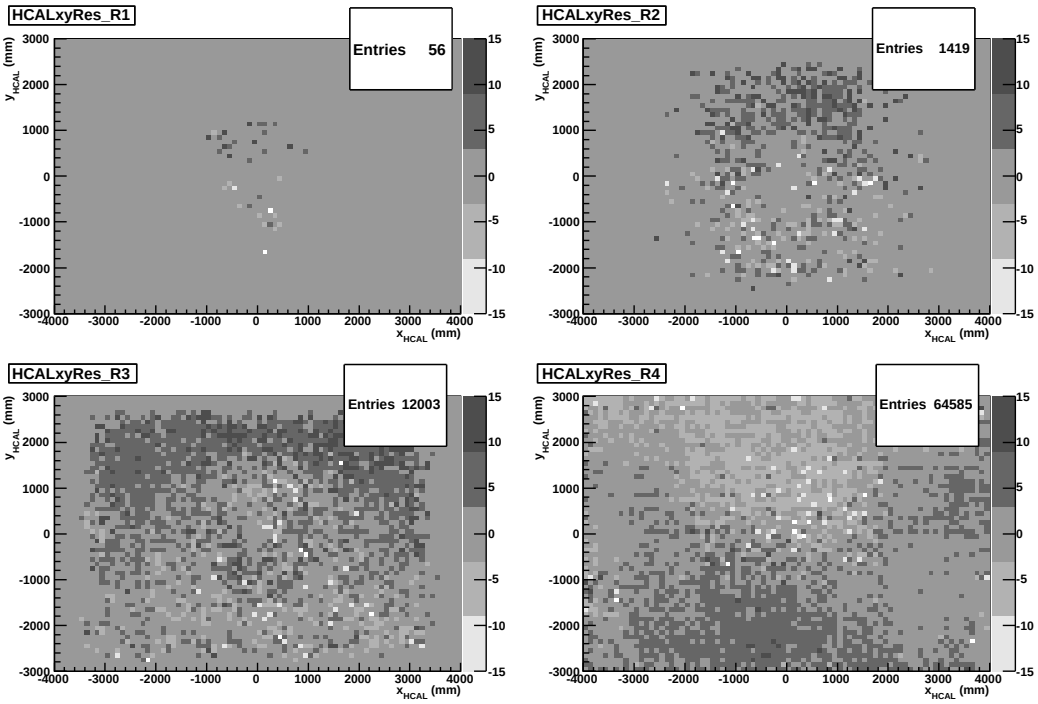

Figure 12 Maps of mean time residuals on hadron calorimeter. Results are separated with respect to the region of muon detector crossed by the track. The color scale is in ns.

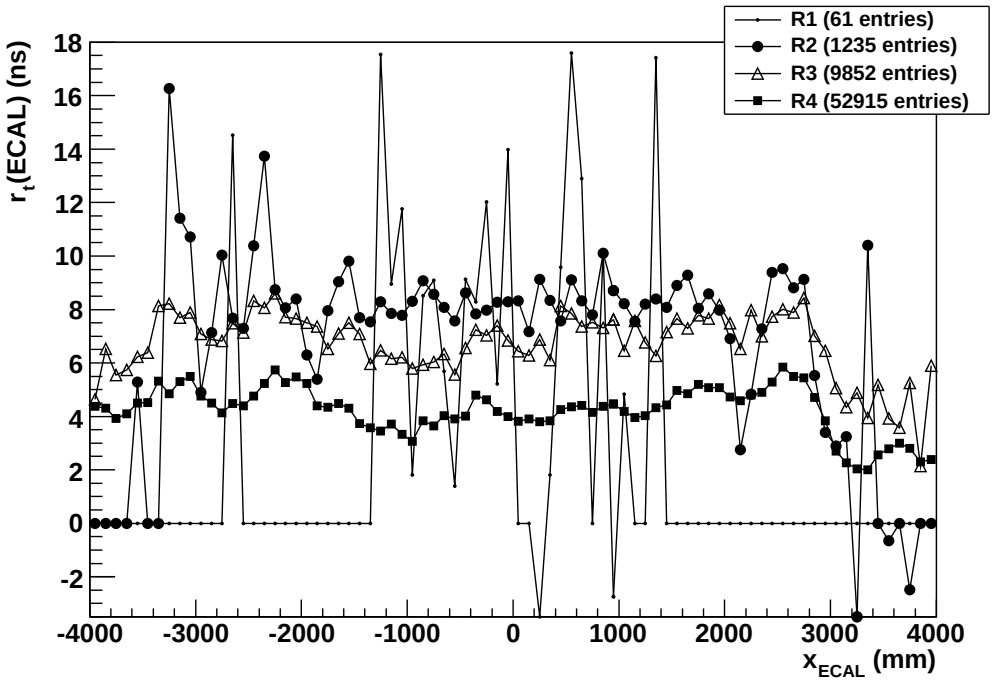

Figure 13 Mean time residual between electromagnetic calorimeter and muon detector versus x coordinate of intersection point.

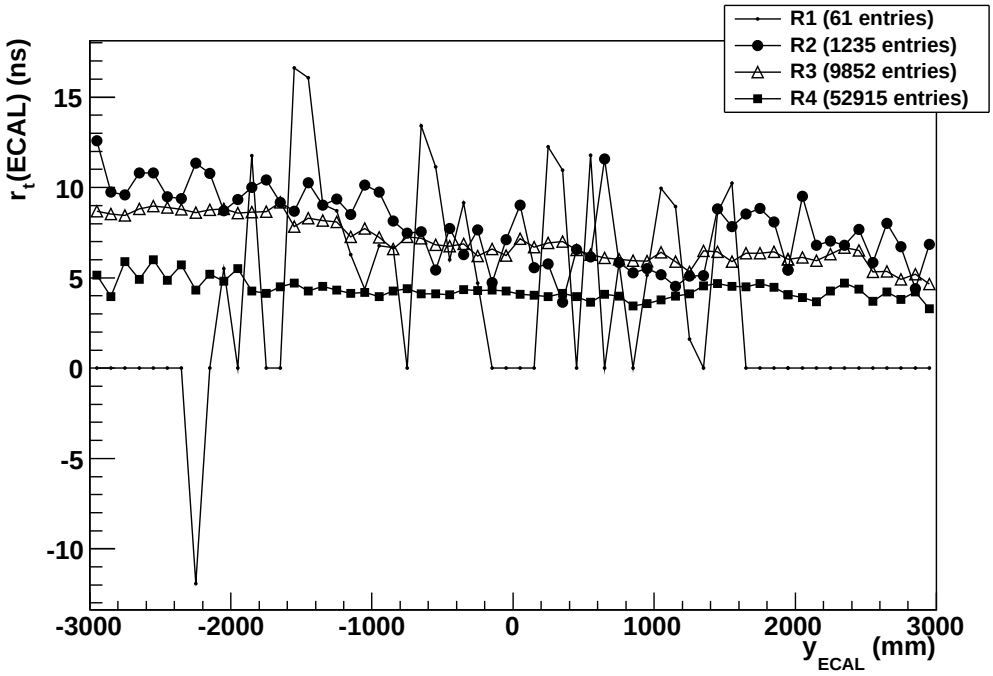

Figure 14 Mean time residual between electromagnetic calorimeter and muon detector versus y coordinate of intersection point.

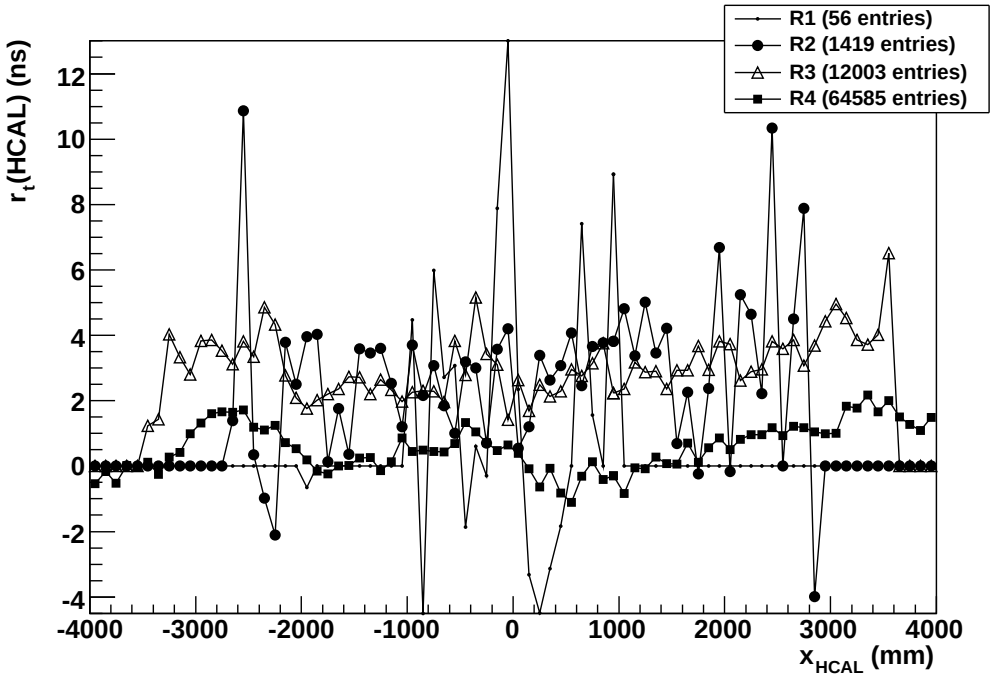

Figure 15 Mean time residual between hadron calorimeter and muon detector versus x coordinate of intersection point.

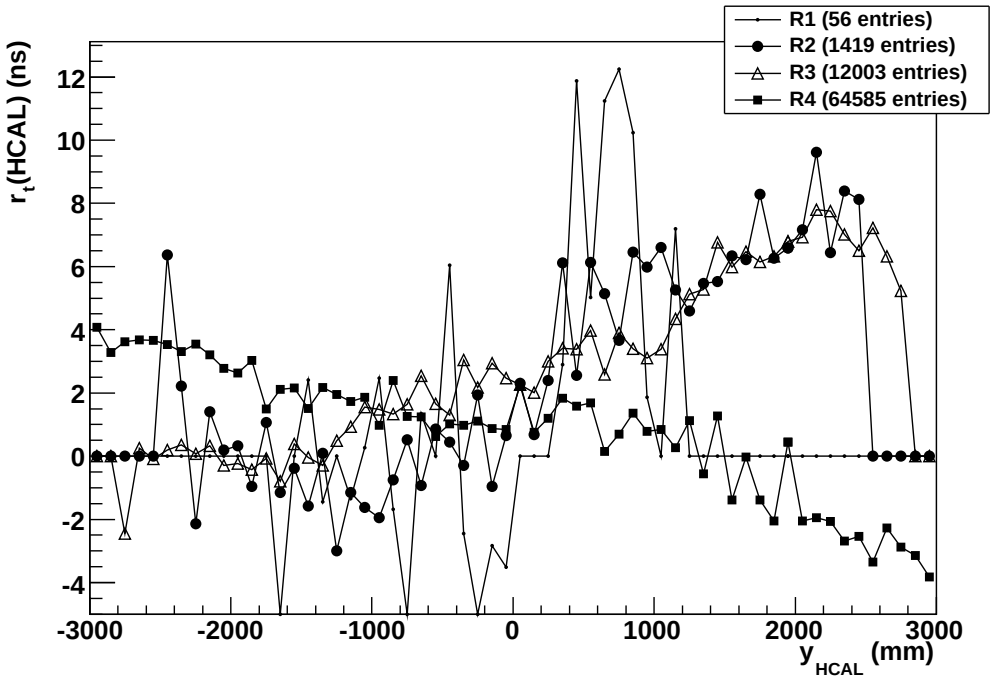

Figure 16 Mean time residual between hadronic calorimeter and muon detector versus y coordinate of intersection point.